Available online at www.sciencedirect.com

ScienceDirect

Mendeleev Commun., 2018, **28**, 110–112

Mendeleev Communications

Self-assembled structures based on rare earth element salts in the interfacial layer of a liquid/liquid system

Elena N. Golubina,* Nikolai F. Kizim, Evgeniya V. Sinyugina and Ilya N. Chernyshev

Novomoskovsk Institute of D. I. Mendeleev University of Chemical Technology of Russia, 301665 Novomoskovsk, Tula Region, Russian Federation. Fax: +7 48762 44695; e-mail: Elena-Golubina@mail.ru, nphk@mail.ru

DOI: 10.1016/j.mencom.2018.01.038

The properties of substance of interfacial structures, which is spontaneously formed in the interfacial layer of a liquid/liquid system upon the extraction of rare earth elements (REEs) with di(2-ethylhexyl)phosphoric acid (D2EHPA) solutions, are mostly determined by the nature of REE and the solvent for D2EHPA. The interfacial substance based on REEs of the yttrium subgroup has higher density, magnetic susceptibility, conductivity and hydrophobicity.

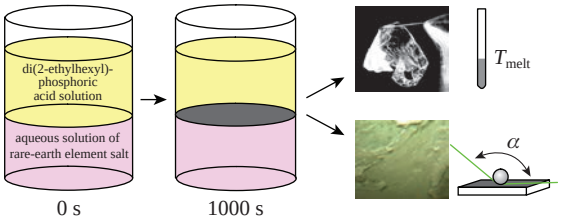

The processes of self-assembly and self-organization in a complex organized system can result in spontaneous formation of ordered structures with practically important properties. The synthesis in space-limited colloidal systems (so-called nanoreactors) is the most common 'bottom-up' method for synthesizing nanostructures. Reverse micelles, adsorption layers, and microemulsions are generally used as the colloidal nanoreactors.[1–4]

The thin films of nanoparticles produced *in situ* at an interface of two immiscible liquids were reported.[5,6] Lin *et al.*[7] synthesized the assemblies of CdSe and CdTe nanoparticles with a specified size at the water/toluene interface. Reincke *et al.*[8] described an Au-NPs hydrophilic system formed on the water/heptane interface stabilized by a citric acid salt, to produce a densely packed monolayer. A method to generate two-dimensional or three-dimensional ordered structures consisting of hydrophobic and hydrophilic nanoparticles synthesized at the water/oil interface was reported.[6,7] Wang *et al.*[9,10] showed that nanoparticles were localized at the water/oil interface.

The water/oil systems are used in solvent extraction. A specific feature of these systems is that upon contact of phases, *viz.* an aqueous solution of a rare earth element (REE) and a di(2-ethylhexyl)phosphoric acid (D2EHPA) solution in an organic solvent, a normal di(2-ethylhexyl)phosphate lanthanide salt, or basic salts at higher pH, are formed spontaneously. They can be accumulated in the interfacial layer to generate nanoparticles forming the basis for structures with specified properties.

Previously,[11–13] we examined some properties of the interfacial substance formed in the above extraction system. Here, we describe the new properties found for these materials.

The REE extraction with a D2EHPA (HR) solution in organic solvents at low pH resulted in the formation of lanthanide di(2-ethylhexyl)phosphate:

$$LnA_3 + 3HR \leftrightarrow LnR_3 + 3HA \quad (1)$$

Under sufficiently high pH in aqueous solutions, the lanthanide salt underwent hydrolysis to produce basic salts in the interfacial layer:

$$Ln(OH)_n^{3-n} + (3-n)HR \leftrightarrow Ln(OH)_nR_{3-n} + (3-n)H^+ \quad (2)$$

Reactions (1) and (2) occur in the interfacial layer if the ratio between the initial concentration of Ln^{III} in the aqueous phase and that of HR in the organic phase is close to stoichiometric. The resulting LnR_3 and $Ln(OH)_nR_{3-n}$ salts are insoluble in both water and an organic phase, and they accumulate in the interfacial region to form a dynamic interfacial layer (DIL). The salt molecules rapidly react with HR and water to generate new phase particles that coalesce and form a spatial grid. Di(2-ethylhexyl)phosphate lanthanide salts slightly soluble in both aqueous and organic phases can subsequently produce an organogel and interfacial precipitates. At low REE concentration (in the initial aqueous phase) and D2EHPA concentration (in organic phase) higher by a factor of 3–5 than that of the REE, the reaction zone is extended towards the aqueous phase due to D2EHPA penetration into these layers. In this case, a significant fraction of the resulting particles of new phase, which are distant from the interface, fails to be retained in the interfacial region and undergoes precipitation. At high REE concentrations and extractant concentrations lower by a factor of 2–5 than those of element being extracted, the reaction front is located near the interface and an interfacial film is formed in the system. The system is stabilized by D2EHPA that possesses surfactant properties and can be adsorbed at the interface.†

The self-assembled structure is formed upon the extraction of REEs due to coagulation and polymerization caused by the crosslinking of lanthanide di(2-ethylhexyl)phosphate molecules.

This fact is indicated by an increase in the absorption in the IR spectra of interfacial substance at 1180 and 1090 cm^{-1} attributed

† A pure REE salt solution (0.1 M, 8 ml) was placed in a conic cell. The interface surface area was 6.07 cm^2. A platinum ring (0.3 cm in diameter) was placed at the solution/air interface. The ring was shaped at the end of a platinum wire (0.1 cm in diameter) with an appropriate length. The ring plane was arranged at the interface normally with respect to the rest of the wire. After that, D2EHPA (88%, purified in accordance with ref. 14) solution (0.05 M, 2 ml) was carefully added along the cell wall. In a certain period of time, the platinum ring containing a fragment of the interfacial structure was carefully and slowly withdrawn from the system. The fragment was washed with water and with a solvent, dried and transferred to a weighing bottle.[11,12]

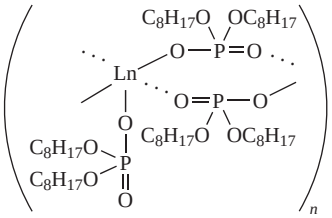

to the ν_{as}(PO) and ν_{s}(PO) vibrations of bridging alkylphosphate groups in linear polymers, respectively.[11]

Changing its appearance with time, the interfacial substance is observed visually and can contract, expand or shrink (Figure 1). It can be removed from the interfacial layer [Figure 2(*a*)] and transferred onto a substrate, such as glass [Figure 2(*b*)], then washed, dried, and analyzed.

According to powder X-ray diffraction study, the interfacial substance based on lanthanide di(2-ethylhexyl)phosphate is non-uniform, areas with amorphous and condensation structures can be observed. In a condensation structure, the di(2-ethylhexyl)-phosphates of lanthanides are isostructural and form a crystal lattice in hexagonal syngony. Linear polymers in which the edges

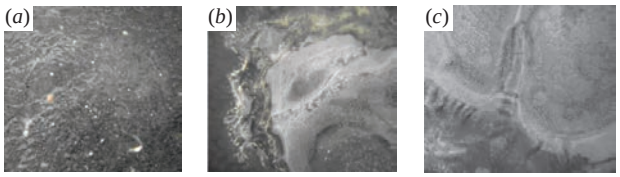

Figure 1 Microscopic images of an interfacial substance at different times from the start of the experiment for the system involving Er^{III} aqueous solution (0.1 M, pH 5.3) and D2EHPA solution in heptane (0.05 M). Time: (*a*) 480, (*b*) 1000 and (*c*) 1200 s.

After isolation of the interface fragment mostly containing lanthanide salts of D2EHPA, the interface was regenerated and the substance was formed again. Interface fragments can be removed repeatedly, as long as the system contains reagents to generate a lanthanide salt of D2EHPA.

Their X-ray diffraction patterns of the interfacial substance were recorded using a DRON-3 diffractometer with CuKα-radiation and a graphite monochromator on the reflected beam. The mean size of crystallites (coherent scattering regions) was estimated using the Selyakov–Scherrer equation.

The IR spectra were recorded on an FSM-1201 IR spectrophotometer. The interfacial substance was triturated and compressed in tablets with potassium bromide. The melting points were determined according to a standard procedure. To evaluate the magnetic susceptibility of the interfacial substance, the sample was placed into the magnetic field of a solenoid, and the potential difference (electromotive force) of a Hall sensor was estimated by a high-resistance microvoltmeter. To measure the electrical conductivity of a removed fragment of the interfacial substance, it was applied onto platinum electrodes connected to an Expert-002 conductivity meter.

To estimate the specific density of the interfacial substance, a glass capillary with known mass was densely packed with the test substance and weighed. The packing tightness was visually controlled with a cathetometer to identify possible air spaces. The volume of substance was estimated using a cathetometer.

To determine the wettability of the modified surface, the substance was removed from the interfacial layer. A thin glass plate (24×16×2 mm) was immersed at a slow constant rate (~1 mm s^{-1}), with its narrow end down, through the light phase layer and the interfacial layer into the heavy phase to a depth of 10 mm. The plate was kept in a fixed position for a certain time, then slowly removed from the system. The second application of the material was carried out similarly. A withdrawn fragment of the interface substance was washed with water and an organic solvent. The contact angle was calculated from the cathetometer-measured diameter and height of a water droplet placed on a modified surface.

Statistical treatment of the experimental data showed their repeatability and reproducibility; the error did not exceed 10%.

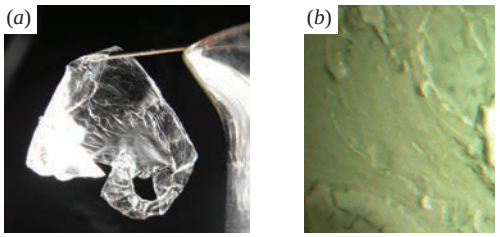

Figure 2 Fragment of interfacial substance (*a*) taken from the interfacial layer of the extraction system and (*b*) transferred onto a glass plate.

are linked by Ln–(O–P–O)$_3$–Ln bridging bonds are the basis of the condensation structure.

Table 1 illustrates the effect of the number of coatings on the contact angle. The second coating increases the hydrophobicity of the modified surface, whereas the third one decreases it. Subsequent 'immersion–removal' of a glass plate, on which the interfacial substance has already been adhesively deposited, through the interfacial zone changes the structure of the surface layer and the water content in it, and hence its wettability. In the series of coatings studied in the systems based on REEs (Pr^{III}, Eu^{III}, Ho^{III}, Er^{III}, Yb^{III}), hydrophobicity was higher in the interfacial substances of yttrium subgroup REEs because of their higher crystallinity. However, a more uniform coating with gelatinous properties was observed for the interfacial substances based on cerium subgroup elements. Note that transition from Pr^{III} to Yb^{III} reduced the water content in the interfacial substance, as confirmed by the lower intensity of the IR spectra at 3480 cm^{-1} (Figure 3).

Table 2 shows that the nature of the element being extracted affects some properties of the materials based on lanthanide di(2-ethylhexyl)phosphates. The temperatures of their melting start are the same and equal to 108 °C. Since the initial and final melting temperatures are different, we can assume that the material is composed of several salts and/or the fraction of polymers changes. The melting points of the materials based on REEs from yttrium subgroup are higher than those of the cerium subgroup due to higher content of a crystalline phase, as confirmed by X-ray diffraction analysis.

Table 1 The contact angle 60 min after the test start.[a]

Lanthanide	Contact angle/deg		
	1 layer	2 layers	3 layers
Pr^{III}	80±3	86±2	82±2
Eu^{III}	84±3	91±2	87±3
Gd^{III}	105±4	122±3	120±3
Ho^{III}	129±2	148±3	142±3
Yb^{III}	132±2	155±2	137±3

[a] 0.1 M aqueous solution of lanthanide, pH 5.3 / 0.05 M D2EHPA in heptane.

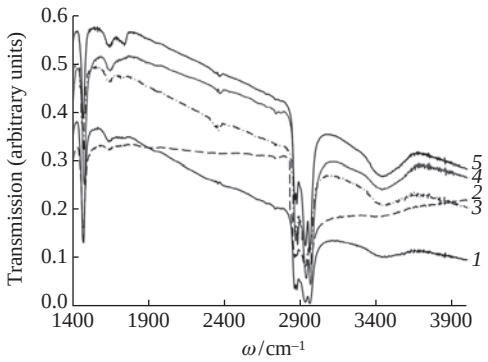

Figure 3 IR spectra of interfacial substance based on di(2-ethylhexyl)-phosphate lanthanides: (*1*) Pr^{III}, (*2*) Eu^{III}, (*3*) Gd^{III}, (*4*) Ho^{III}, and (*5*) Yb^{III}.

Table 2 Effect of the REE nature on the properties of interfacial substances.[a]

Lanthanide	Melting point / °C	Conductivity / μS	Magnetic susceptibility / $cm^3\ mol^{-1}$	Density / g cm^{-3}	Crystallite size / nm	Degree of crystallinity (%)
Pr^{III}	112 ± 0.5	0.047 ± 0.003	0.0235 ± 0.004	2.03 ± 0.07	40.3–64.1	18.7
Eu^{III}	114 ± 0.5	0.074 ± 0.005	0.0243 ± 0.005	2.31 ± 0.07	27.6–36.5	22.7
Gd^{III}	114 ± 0.5	0.082 ± 0.005	0.0251 ± 0.004	3.44 ± 0.08	20.5–29.2	23.5
Ho^{III}	115 ± 0.5	0.120 ± 0.008	0.0313 ± 0.005	3.24 ± 0.09	21.5–27.0	25.8
Yb^{III}	120 ± 0.5	0.142 ± 0.008	0.0355 ± 0.005	3.74 ± 0.10	18.0–18.8	27.3

[a] 0.1 M aqueous solution of lanthanide, pH 5.3 / 0.05 M D2EHPA in heptane.

Table 3 Effect of the solvent for D2EHPA on the properties of the interfacial substance.[a]

Solvent	mp / °C	Magnetic susceptibility / $cm^3\ mol^{-1}$	Specific density / g cm^{-3}	Contact angle[b] / deg	Crystallite size / nm	Degree of crystallinity (%)
Hexane	110 ± 0.5	0.0313 ± 0.005	3.83 ± 0.12	94 ± 2	16.2–22.9	29.8
Heptane	115 ± 0.5	0.0308 ± 0.005	3.24 ± 0.09	95 ± 2	21.5–27.0	25.8
Octane	130 ± 0.5	0.0283 ± 0.005	2.54 ± 0.13	115 ± 2	25.5–26.0	21.8
Nonane	142.5 ± 0.7	0.0278 ± 0.005	2.25 ± 0.10	125 ± 3	28.2–33.3	18.7
Decane	158 ± 0.7	0.0275 ± 0.005	1.93 ± 0.12	133 ± 2	37.6–43.2	13.3

[a] 0.1 M aqueous solution of Ho^{III}, pH 5.3 / 0.05 M solution of D2EHPA. [b] Data refer to 20 min of contact between the phases.

The conductivity of the interfacial substance taken from the interfacial layer and applied to electrodes is low and depends on many factors. It is related to water content in the material, as supported by changes of absorption intensity at 3480 cm^{-1} in the IR spectra.

The magnetic properties of the materials based on REEs are determined by the unfilled 4*f*-subshell ($4f^n 5s^2 5p^6 5d^{0(1)} 6s^2$, n = 1–14) shielded from the effects of the crystal field by the overlying $5s^2$, $5p^6$ and $5d^{0(1)}$ electron layers. The orbital moment is 'frozen' by the crystal field, *i.e.* its direction cannot be changed by external magnetic field.[15] The increase in the number of 4*f* electrons on transition from lanthanum to lutetium determines a monotonic increase in their magnetic susceptibility (see Table 2).

The magnetic moments are determined by the orbital (L) and spin (S) electron properties. According to Hund's rule, when the electron shells are filled, $J = L - S$ for the cerium subgroup elements, while $J = L + S$ for the yttrium subgroup. Therefore, the orbital and spin moments of ions and atoms of the REE from cerium subgroup should be oriented towards each other, whereas for those of REE from yttrium subgroup, the spin and orbital moments must be parallel. Hence, materials based on the REE from cerium subgroup are expected to possess smaller magnetic moments and lower magnetic susceptibility than those from the yttrium subgroup.[15]

On transition from hexane to decane in the series of solvents for D2EHPA, the crystallinity fraction and the crystallite size change (Table 3), resulting in a material based on lanthanide di(2-ethylhexyl)phosphate with lower density and smaller magnetic susceptibility but higher melting temperature. The effect of reduced crystallite size on the melting point can be attributed to the surface pressure[16] acting on the material. This additional pressure, which is inversely proportional to the particle size, releases additional Gibbs free energy. As a result, the melting point decreases. Note that the crystal lattice type of interfacial substance does not change, whereas the ratio of crystallographic axes (c/a) does change, which affects the magnetic susceptibility.

The water content in the interfacial substance decreases (lower intensity in the IR spectra at 3480 cm^{-1}) on the transition from hexane to decane. The fraction of linear polymer in the material changes, as evidenced by the variability of the line intensity at 1180 and 1090 cm^{-1} in the IR spectra. The crystallite size, water content, and fraction of polymers all contribute to the properties of interfacial substance.

Thus, the interfacial substance that is spontaneously formed in the interfacial layer of the liquid/liquid system upon the REE extraction by D2EHPA reveals the properties mostly determined by the REE nature and the type of solvent for D2EHPA. The interfacial substance based on yttrium subgroup REEs possesses higher density, magnetic susceptibility, conductivity and hydrophobicity.

References

1 A. A. Eliseev and A. V. Lukashin, *Funktsional'nye nanomaterialy (Functional Nanomaterials)*, ed. Yu. D. Tret'yakov, Fizmatlit, Moscow, 2010 (in Russian).
2 M. Yu. Koroleva, T. Yu. Nagovitsina and E. V. Yurtov, *Mendeleev Commun.*, 2015, **25**, 389.
3 L. Ya. Zakharova, R. R. Kashapov, T. N. Pashirova, A. B. Mirgorodskaya and O. G. Sinyashin, *Mendeleev Commun.*, 2016, **26**, 457.
4 C. Solans and I. Solé, *Curr. Opin. Colloid Interface Sci.*, 2012, **17**, 246.
5 D. Yogev and S. Efrima, *J. Phys. Chem.*, 1988, **92**, 5754.
6 C. N. R. Rao, G. U. Kulkarni, P. J. Thomas, V. V. Agrawal and P. Saravanan, *J. Phys. Chem. B*, 2003, **107**, 7391.
7 Y. Lin, H. Skaff, T. Emrick, A. D. Dinsmore and T. P. Russell, *Science*, 2003, **299**, 226.
8 F. Reincke, S. G. Hickey, W. K. Kegel and D. Vanmaekelbergh, *Angew. Chem. Int. Ed.*, 2004, **43**, 458.
9 H. Duan, D. Wang, D. G. Kurth and H. Möhward, *Angew. Chem. Int. Ed.*, 2004, **43**, 5639.
10 Z. Mao, J. Guo, S. Bai, T. L. Nguyen, H. Xia, Y. Huang, P. Mulvaney and D. Wang, *Angew. Chem. Int. Ed.*, 2009, **48**, 4953.
11 N. F. Kizim, E. N. Golubina and A. M. Chekmarev, *Russ. J. Phys. Chem. A*, 2013, **87**, 502 (*Zh. Fiz. Khim.*, 2013, **87**, 517).
12 E. N. Golubina, N. F. Kizim and A. M. Chekmarev, *Russ. J. Phys. Chem. A*, 2014, **88**, 1594 (*Zh. Fiz. Khim.*, 2014, **88**, 1427).
13 N. F. Kizim and E. N. Golubina, *Radiochemistry*, 2016, **58**, 287 (*Radiokhimiya*, 2016, **58**, 248).
14 W. J. McDowell, P. T. Perdue and G. N. Case, *J. Inorg. Nucl. Chem.*, 1976, **38**, 2127.
15 A. A. Preobrazhensky and E. G. Bishard, *Magnitnye materialy i elementy (Magnetic Materials and Elements)*, Vysshaya Shkola, Moscow, 1986 (in Russian).
16 G. B. Sergeev, *Nanokhimiya (Nanochemistry)*, MGU, Moscow, 2007 (in Russian).

Received: 13th February 2017; Com. 17/5176